Axisymmetric intrusions in two-layer and uniformly stratified environments with and without rotation

Amber M. Holdsworth,[1] Kai J. Barrett,[2] and Bruce R. Sutherland[1,2,a)]
[1]*Department of Earth & Atmospheric Sciences, University of Alberta, Edmonton, Alberta T6G 2E3, Canada*
[2]*Department of Physics, University of Alberta, Edmonton, Alberta T6G 2E1, Canada*

(Received 3 August 2011; accepted 13 February 2012; published online 26 March 2012)

Lock-release laboratory experiments have been performed to examine the collapse of a localized cylindrical mixed patch of fluid in both two-layer and uniformly stratified ambients. The experiments were performed with and without rotation. Unlike bottom propagating gravity currents, non-rotating intrusions typically propagated many lock radii at constant speed, sometimes stopping abruptly due to interactions with internal waves generated by the return flow into the lock. The initial front speeds of the resulting approximately axisymmetric intrusions emanating from locks of comparable depth and radius were found to be 30%–35% less than the predictions of rectilinear theory. Rotation had no impact on the intrusion's initial speed. However, it limited the maximum distance propagated by the intrusion and caused the patch to expand and contract as it approached geostrophic balance. © *2012 American Institute of Physics*. [http://dx.doi.org/10.1063/1.3696018]

I. INTRODUCTION

Driven by differences in density, a gravity current forms when fluid of uniform density flows horizontally into fluid of a different density or into density stratified fluid. In the latter case the current can propagate within the interior of the fluid along its level of neutral buoyancy as an intrusive gravity current or, simply, an intrusion.

Stratified fluids support internal waves which move due to buoyancy forces transporting both energy and momentum. When these waves are confined to an interface, as is the case in a two-layer fluid, they are called interfacial waves. In a continuously stratified fluid internal waves can propagate vertically as well as horizontally.

In the ocean and atmosphere, turbulence generated by breaking internal waves, shear instabilities and convection can mix the stratified ambient generating a patch of uniform density fluid. When a turbulent mixing event occurs near a pycnocline the collapse of the patch can lead to the formation of an intrusion and an associated interfacial wave that propagates along the pycnocline.[1] If the motion is sufficiently long in time and space, the Earth's rotation can additionally influence the evolution.

Understanding the evolution of these localized density anomalies provides motivation for the laboratory experiments presented here.

Most theoretical and experimental studies of gravity currents have assumed that a constant volume is released from a lock in a rectilinear geometry.[2–4] Gravity currents are known to propagate at near-constant speed, as predicted by Benjamin,[5] for 6–10 lock lengths.[6] Thereafter, in what is called the self-similar regime, the speed is predicted to decrease as the head height of the current decreases.[7]

Theoretical predictions of the initial speed of the intrusion have been established for both two-layer[8] and uniformly stratified[9] ambients. Experiments have shown that the evolution of rectilinear intrusions is significantly altered by the generation of and interaction with internal waves.[10–13]

a)Email: bruce.sutherland@ualberta.ca. URL: http://www.ualberta.ca/~bsuther.

In a two-layer and uniformly stratified ambient, symmetric intrusions were observed to propagate at near-constant speed well beyond 10 lock lengths[13,14] without entering the self-similar regime. For thick interfaces the intrusion evolved into a mode-2 closed core solitary wave which carried the intrusion forward despite a continuous decrease in the intrusion's head height. Rather than being slowed by a rear-shock, asymmetric intrusions were entirely halted when mode-1 internal waves which were launched by the return flow that reflected off the lock end of the tank caught up to the intrusion's head.

There have been relatively few studies examining the speed of gravity currents released from a cylinder and spreading circularly. This is because the geometry dictates the head must decelerate shortly after release. However, recent studies[13–15] showed that vertically symmetric intrusions propagate at constant speed even though their head heights decrease. This result motivated the present investigation into the evolution of non-vertically symmetric axisymmetric intrusions in two-layer and uniformly stratified ambients. Finding that the intrusion speed is constant for many lock radii we focus upon measuring the intrusion speeds and compare these with the predicted rectilinear speed.

A brief review of theory for intrusions is given in Sec. II. The experimental set-up and the methods used to analyze the intrusion speeds are presented in Sec. III with the results shown in Sec. IV. Conclusions are given in Sec. V.

II. BACKGROUND AND THEORY

A. Rectilinear intrusions

Numerous studies have examined spanwise uniform gravity currents propagating beneath a uniform ambient. Benjamin[5] predicted that the speed for a steady Boussinesq current of density $\rho_{\mathcal{C}}$ propagating beneath a uniform ambient of density ρ_a is given by

$$U = \frac{1}{2}\sqrt{g'H}, \tag{1}$$

where $g' \equiv g(\rho_{\mathcal{C}} - \rho_a)/\rho_0$ is the reduced gravity, g is gravity, ρ_0 is the characteristic density, H is the total depth of the fluid, and Fr is the dimensionless Froude number.

In lock-release laboratory experiments, fluid of one density $\rho_{\mathcal{C}}$ is partitioned from fluid of another density ρ_a by a thin gate. When the gate is removed the lock-fluid collapses under the influence of gravity. After the relatively brief "slumping phase" the current propagates along the bottom boundary at near-constant speed.

Lock exchange experiments have also been used to study intrusions of uniform density, $\rho_{\mathcal{C}}$, in a two-layer ambient fluid with an upper (lower) layer density ρ_{U} (ρ_{L}) of depth h_{U} (h_{L}).

The speed of the intrusions may be characterized by two independent non-dimensional parameters, ϵ and Δ. The relative density difference between the intrusion and the average density of the ambient is represented by

$$\epsilon \equiv \frac{\rho_{\mathcal{C}} - \langle\rho\rangle}{\rho_L - \rho_U}, \tag{2}$$

where

$$\langle\rho\rangle \equiv \frac{h_{\mathrm{U}}\rho_{\mathrm{U}} + h_{\mathrm{L}}\rho_{\mathrm{L}}}{H} \tag{3}$$

is the depth-weighted average ambient density.

The relative difference between the upper and lower layer depths is represented by

$$\Delta \equiv \frac{(h_{\mathrm{U}} - h_{\mathrm{L}})}{H} \tag{4}$$

in which $H = h_{\mathrm{U}} + h_{\mathrm{L}}$.

When $\epsilon = 0$ and $\Delta = 0$, the intrusion is vertically symmetric and equal masses of lock-fluid are transported in each layer. This circumstance has been studied extensively in laboratory experiments.[11,16,17] Following the approach of Benjamin,[5] Holyer and Huppert[11] made the first prediction of intrusion speeds in vertically asymmetric cases with ϵ and/or Δ non-zero. However,

Sutherland *et al.*[18] found that the theory was in agreement with their experiments for intrusions only if $\epsilon = 0$. If ϵ differed moderately from zero, the theory significantly underpredicted the speeds.

When $\epsilon \neq 0$ the interface ahead of the intrusion was depressed or elevated by the intrusion. This generated a long interfacial wave that propagated ahead of the intrusion. Based upon this observation Benjamin's theory was adapted to account for the displaced interface.[8,19] Recasting the formula for the speed in terms of ϵ and Δ gives

$$U_{2L} = \frac{1}{4}\sqrt{g'H}\sqrt{1 - \Delta^2 + 4\Delta\epsilon}, \tag{5}$$

where $g' \equiv (\rho_L - \rho_U)/\rho_0$.

Ungarish *et al.*[7] used shallow water theory to predict the speed of gravity currents beneath uniformly stratified ambient. However, by requiring the flow to be hydrostatic, the theory could not be extended to intrusions which excite non-hydrostatic internal waves.[13]

Following the approach of Cheong *et al.*,[19] Bolster *et al.*[9] predicted the speed of intrusions in uniformly stratified fluid with buoyancy frequency $N = \sqrt{(-g/\rho_0)(d\bar{\rho}/dz)}$, in which $\bar{\rho}$ is the background density profile. Their formula was recast in terms of ϵ by Munroe *et al.*[13] to give

$$U_N = \frac{1}{4}NH\sqrt{3\epsilon^2 + \frac{1}{4}}. \tag{6}$$

Here ϵ is given by Eq. (2) where ρ_L corresponds to the density at the bottom and ρ_U corresponds to the density at the fluid's surface and $\langle\rho\rangle$ is the average of the two densities.

In partial-depth lock-release experiments[12] in uniformly stratified fluid the intrusion was found to evolve as if released from a full-depth lock in a tank of depth H_m in which H_m is height of the mixed lock-fluid. Taking $\epsilon = 0$ and $H = H_m$ in Eq. (6), the speed is given by

$$U_{NP} = \frac{1}{8}NH_m. \tag{7}$$

This result agrees with the experimentally determined Froude number[12] of $U/NH_m = (0.13 \pm 0.02)$.

B. Axisymmetric intrusions

The results above were determined in a rectilinear geometry. In an axisymmetric geometry, by conservation of mass, the widening circumference of the radial spreading intrusion reduces the intrusion's head height and so should decrease the intrusion's speed.

Huppert and Simpson[3] noted that the gravity current moved at near-constant speed for short times and predicted that the position of the front changed proportionally to $t^{1/2}$ during the self-similar regime. This regime was observed to establish itself after propagating approximately 3 lock-radii.

Sutherland and Nault[14] studied the effect of interface thickness on the intrusion's speed in the vertically symmetric two-layer case ($\epsilon = \Delta = 0$). They noted that the front of the intrusion was more corrugated than its rectilinear counterpart, but it propagated at near-constant speed beyond 8 lock radii.

Using a combination of laboratory experiments and numerical modelling, McMillan and Sutherland[15] found that the non-zero thickness of the interface resulted in a mode-2 solitary wave that surrounded the intrusion head and carried it radially outwards. This caused the current to move at near-constant speed even as the wave amplitude decreased with radial distance as $r^{-1/2}$. The speed of the intrusions in vertically asymmetric and axisymmetric circumstances have not been examined in detail.

In uniformly stratified fluid, most laboratory experiments have examined axisymmetric intrusions resulting from continuous forcing of a turbulent patch.[20–22] The only lock-release experiments were performed by Holdsworth *et al.*[23] This study focused upon internal waves generated by the collapse of a partial-depth lock and did not focus on the speed and evolution of the intrusion itself.

C. Influence of rotation

A combination of laboratory experiments and numerical modelling have been used to investigate the axisymmetric spreading of rotating bottom-propagating gravity currents in uniform density ambient.[24–26] The horizontal distance at which rotation becomes as important as buoyancy is given by the (internal) Rossby deformation radius,

$$L_D = U_c/f_0. \tag{8}$$

The characteristic velocity, U_c, used for the two-layer and uniformly stratified cases were taken from Eqs. (5) and (6), respectively, with Eq. (7) being used for partial-depth lock-release experiments.

The Rossby number describes the relative importance of inertia to rotation and is given by

$$\mathrm{Ro} = L_D/R_c, \tag{9}$$

where R_c is the radius of the cylindrical lock and L_D is defined by Eq. (8). Thus, Ro is defined *a priori*, in terms of the independent experimental parameters, rather than from measured quantities.

For $\mathrm{Ro} \gg 1$ inertial forces dominate and the adjustment of the patch is expected to behave similarly to the non-rotating case. However, for small values of the Rossby number, $\mathrm{Ro} \ll 1$, the current is expected to be influenced by rotation during the slumping phase and then rapidly adjust to geostrophic balance.

The geostrophic adjustment of an isolated axisymmetric lens was studied by Stuart *et al.*[27] using a combination of experiments and numerical models. They focused on the dependence of the velocity and length-scale of the adjustment on the Burger number, $\mathrm{Bu} = \mathrm{Ro}^2$. Finding that the velocities scaled with the reduced gravity wave speed and the adjustment distance scaled with the Rossby deformation radius of the patch. This study and others[28] characterized properties of the lens and its relationship with initial conditions. The present study of rotating intrusions focuses, instead, on the speed of the intrusion and its interaction with interfacial waves immediately following its release from the lock, for the most part in experiments with Rossby number order unity and higher.

In their study of bottom propagating gravity currents in uniform ambients, Hallworth *et al.*[25] found that rotating currents stopped after propagating a finite radius unlike their non-rotating equivalents. For large Reynolds numbers the currents initially propagated out radially to a distance of 3.7–5.5 lock radii. The ratio of $R_{\max}/L_D$ ranged from 3.7 to 5.1 for Rossby numbers between 0.6 and 1.5.

Once $R_{\max}$ was reached the flow reversed direction and the majority of the current accumulated near the centre of the tank. The mass of fluid then exhibited a second outward pulse which propagated outward radially and often exceeded $R_{\max}$ by a short distance. The frequency of the pulsations increased with the rotation rate of the fluid according to $\omega_p = 2.10\Omega$. This result was independent of the initial conditions indicating that the pulsations were a result of inertial oscillations.

Ungarish and Huppert[29] used a one-layer shallow water approximation to analyze gravity currents propagating beneath a uniformly stratified ambient. They compared their results with Navier-Stokes simulations and available experiments.[4,25] They found that gravity currents propagating beneath a uniformly stratified ambient had a lower initial speed and shorter distance of propagation than the homogeneous case. Consistent with previous studies of gravity currents in uniform ambients[24] they found that the current rotated anticyclonically. The strength of the counter-rotation increased with the radial distance propagated by the current from the edge of the cylindrical lock and further restricted $R_{\max}$.

Although some of these ideas may be extended to rotating intrusions, experiments examining these dynamics are reported upon for the first time here.

III. EXPERIMENTAL SETUP

Figure 1 illustrates the laboratory setup for (a) two-layer and (b) uniformly stratified experiments. All experiments were performed in an cylindrical acrylic tank of height $H_T = 30.0$ cm and inner diameter of $D_T = 90.7$ cm. The tank was centred on a Geophysical Fluids Rotating Table by Australian Scientific Instruments which can rotate at frequencies Ω between 0.020 and 15.00 s^{-1}.

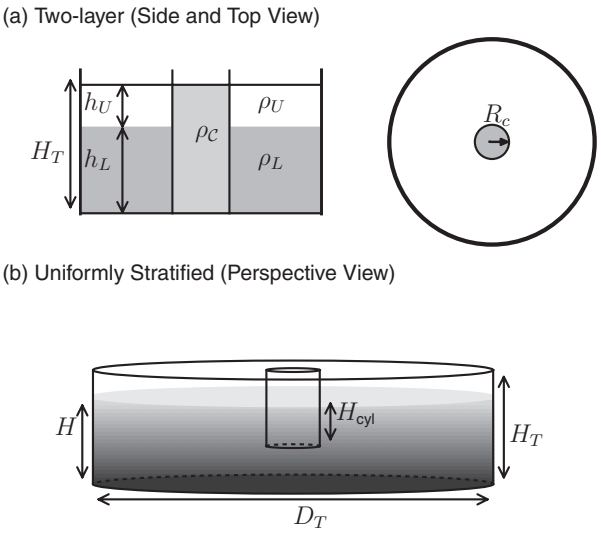

FIG. 1. Experiments were performed in a cylindrical tank of height H_T and inner diameter $D_T = 90.7$ with a hollow cylindrical lock of radius R_c. The tank was filled to a total depth H. (a) The two-layer experiments consisted of a lower (upper) layer depth h_L (h_U) with density ρ_L (ρ_U) and a full-depth lock, whereas in (b) the uniformly stratified experiments the inner cylinder was suspended to a partial-depth H_{cyl}.

A series of experiments were performed while the tank was stationary and another series were performed with the fluid rotating initially in solid body rotation.

A monochrome Cohu CCD camera was situated on a metal frame 2 m directly above the centre of the tank to record a top view of the experiments. From these, time series were constructed showing the radially spreading flow.

As shown in Figure 1(a) the two-layer experiments consisted of a salty lower layer of density ρ_L and height h_L below a freshwater layer of depth h_U and density ρ_U. In all experiments $H = h_L + h_U = 10$ cm was the total depth of the fluid.

For the two-layer experiments, a small amount of dye was added along the interface. Evenly spaced lines at the base of the tank were used to establish an accurate coordinate system.

The experiments were performed shortly after the two-layer stratification was established so as to minimize diffusion across the interface. However, some mixing did occur during the filling stage and resulted in a typical interface half-thickness of $h_\rho \simeq 0.5$ cm.

A hollow acrylic cylinder of radius $R_c = 6$ cm was then carefully inserted in the centre of the tank and extended to the full-depth of the fluid. This formed a lock. The fluid within the lock was mixed so that the density of the fluid ρ_C was the depth-weighted average density of the background fluid. In some of the experiments this density was increased or decreased, respectively, by adding salt or displacing a quantity of fresh water within the cylinder.

A small amount of food coloring was then mixed into the lock to visualize the intrusion. Density measurements indicated that the dye did not significantly affect the density of the lock-fluid. After the turbulence from mixing the lock-fluid had dissipated the cylinder was rapidly extracted vertically using a string and pulley system that helped ensure a vertical extraction.

We explored a range of density configurations characterized by the experimental parameters $\Delta \leq |0.667|$ and $\epsilon \in (-0.237, 0.675)$. The Reynolds numbers, $\mathrm{Re} = U_{2L}H/\nu$, ranged from 2×10^3 to 1×10^4. In the rotating two-layer experiments the rotation rates ranged from of $\Omega = 0.05\,\mathrm{s}^{-1}$ to $\Omega = 0.2\,\mathrm{s}^{-1}$.

Figure 1(b) shows the experimental setup for the continuously stratified fluid experiments. The tank was filled with salt stratified fluid to a depth H (between 17 cm and 19 cm) using the standard "Double-Bucket" technique.[30] For experiments with rotation, the water in the buckets was allowed to reach room temperature before filling the tank to minimize the effects of double diffusion during

the lengthy spin-up process. Measurements of the density were taken at several heights to verify that the background density increased linearly with increasing depth. Linear regression was then applied to the measurements of the ambient density profile, $\bar{\rho}(z)$, to find the density gradient. From this we determined the buoyancy frequency, which ranged from $N = 0.53\,\mathrm{s}^{-1}$ to $2.27\,\mathrm{s}^{-1}$.

For the uniformly stratified experiments, a grid of evenly spaced lines placed at the top of the fluid was used to establish the world coordinates at the level of the intrusion by making a simple adjustment for the index of refraction using Snell's law.

The partial-depth mixed layer, H_m, could be measured visually from side views before the start of an experiment. To determine H_m more accurately, measurements were taken of the density of the lock-fluid, $\rho_{\mathcal{C}}$. In combination with the measured density profile, $\rho_{\mathcal{C}}$ was used to compute the depth below the surface $z_{\mathcal{C}} = H_m/2$, at which the intrusion propagated along its level of neutral buoyancy.

The value of ρ_C was not measured directly for all of the stationary experiments. So the measured value of H_m was used instead for the non-rotating cases.

Taking care not to disturb the ambient stratification, a hollow acrylic cylinder of radius $R_c = 5.3$ cm was inserted into the centre of the tank and suspended at depth H_{cyl}. The fluid within the transparent cylinder was then mixed with a torsionally oscillating mechanical stirrer to a depth H_m, moderately smaller than H_{cyl}. To examine the effect of varying the mixed-region depth we examined a range of experiments with H_m between 2 cm and the full-depth of the fluid, H.

Like the two-layer fluid experiments, the lock-fluid was dyed, mixed and the cylinder was extracted once the residual turbulence had vanished. A metal cylinder and rod were used both to suspend and to guide the cylinder during extraction.

For the uniformly stratified fluid experiments the Reynolds number $\mathrm{Re} = N H_m^2/\nu$ ranged from 8.5×10^2 to 7.0×10^4. In the rotating experiments the tank was gradually rotated up to a frequency of $\Omega \in (0.02, 0.3)$. Dye lines ensured that the entire volume of fluid was ultimately in solid body rotation. This spin-up process typically took over 12 h. Measurements of the density profile $\bar{\rho}(z)$ taken before and after spin-up indicated that the stratification was not changed during the spin-up process.

In all of the experiments the intrusion moved at near-constant speed, U, shortly after being released from the lock. Only those experiments in which the intrusion propagated axisymmetrically were analyzed.

An example of a vertically symmetric intrusion moving along a sharp interface in a two-layer fluid ($\epsilon = 0$, $\Delta = 0$) is shown in Figure 2. The top view in (a) shows that the radially spreading intrusion shortly after release from the lock remains nearly axisymmetric. The time series in (b) is

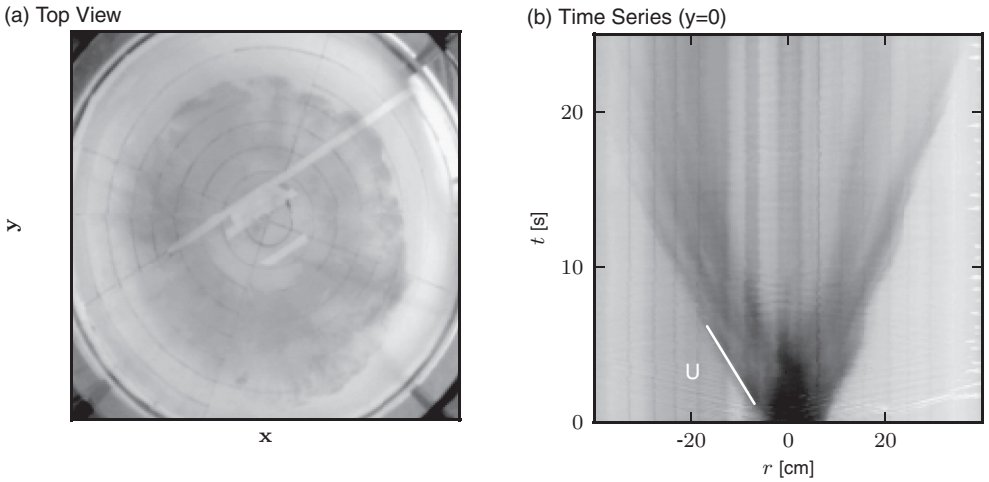

FIG. 2. Two-layer experiment with $\Delta = 0, \epsilon = 0$, $\rho_{\mathrm{L}} = 1.0504\,\mathrm{g/cm}^3$, $\rho_{\mathcal{C}} = 1.0248\,\mathrm{g/cm}^3$ shown from (a) the top view taken when $t \simeq 10$ s and (b) as a time series constructed across the diameter in the x-direction. The slope of the white line shown gives the speed, U, of the current.

constructed across the diameter in the x-direction. This clearly shows the advance of the intrusion head at near-constant speed for at least 6 lock radii.

Figure 2(b) also illustrates how the position of the intrusion head was tracked as it advanced in time. Linear regression was used to obtain a measure of the near-constant speed as the slope of the line shown. Slopes were computed on both sides of the time series. These slopes were then averaged with slopes measured from another time series taken across the diameter in the y-direction. The standard deviation amongst these values was used as an estimate of the error in measurement.

IV. RESULTS

A. Non-rotating experiments

For all the non-rotating experiments, the cylindrical gate was extracted and the lock-fluid collapsed spreading radially outward. Simultaneously return flows above and below the intrusion's head moved inward to replace the lock-fluid. The intrusion propagated outward at near-constant speed for a distance of at least 1.5 lock radii and, for the vertically symmetric two-layer experiments, often exceeded 7 lock radii. In the two-layer experiments the duration of the constant speed regime depended on the parameters ϵ and Δ.

Time series for distinct ϵ and Δ cases are shown in Figure 3. Like the vertically symmetric case shown in Figure 2 when $\epsilon = 0$ and $\Delta \neq 0$ (Figure 3(a)) the intrusion propagated radially at near-constant speed until impacting the side wall of the tank.

When $\epsilon \neq 0$, $\Delta = 0$ the intrusion stalled after propagating a short distance from the lock, slowing to the point of almost stopping. Then it accelerated once more and propagated outward until impacting the tank wall. This stalling behaviour is indicated by the black arrow in the time series in Figure 3(b).

When $\epsilon \neq 0$ and $\Delta \neq 0$ the intrusion's behaviour was remarkably different, as shown in Figure 3(c). The intrusion propagated at near-constant speed a relatively short distance from the lock and then rapidly came to a halt. In some experiments, the intrusion stalled temporarily after propagating some distance from the lock, but then accelerated again moving a short distance again before stopping.

As in the corresponding rectilinear intrusion study,[18] the qualitative features that distinguish the various cases are explained by considering interactions of the intrusion with interfacial waves. When $\epsilon = 0$, a mode-1 interfacial wave is not efficiently excited ahead or behind the intrusion. Instead, a mode-2 interfacial wave surrounds the intrusion head and carries it forward at constant speed even as the head height decreases.[15] The stalling and stopping of the intrusion in cases where $\epsilon \neq 0$ is attributed to interactions of the intrusion with a mode-1 interfacial wave launched by the return flow that enters the lock at different speeds above and below the interface. This vertically asymmetric forcing of the interface launches a large amplitude mode-1 wave that catches up with the intrusion head and stops it.

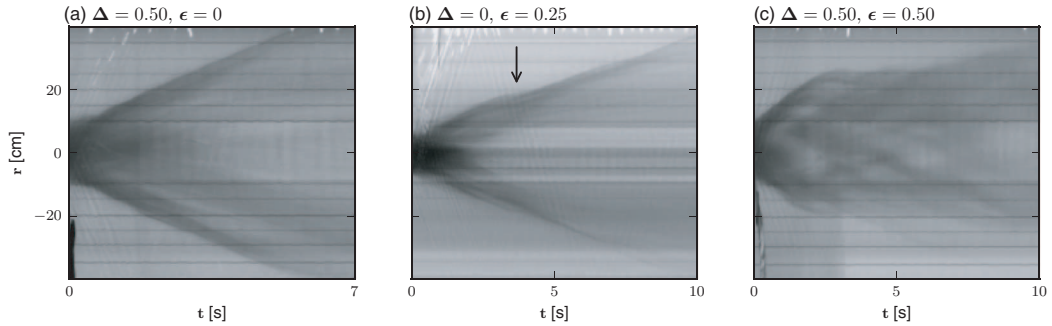

FIG. 3. Time series taken from non-rotating experiments in a two-layer fluid with $H = 10$ cm, $R_c = 6$ cm, and (a) $h_L = 2.5$ cm, $\rho_L = 1.1047$ g/cm^3, $\rho_C = 1.0248$ g/cm^3, (b) $h_L = 5$ cm, $\rho_L = 1.051$ g/cm^3, $\rho_C = 1.0375$ g/cm^3, (c) $h_L = 2.5$ cm, $\rho_L = 1.1047$ g/cm^3, $\rho_C = 1.0781$ g/cm^3.

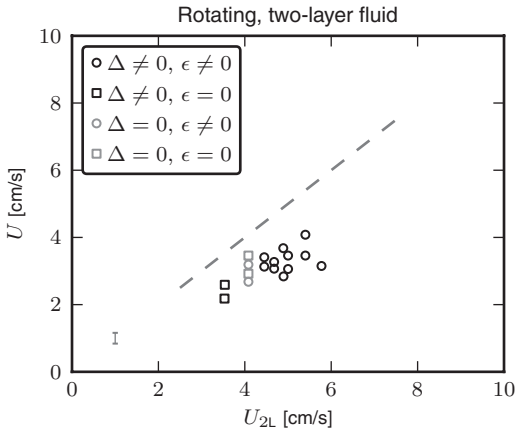

FIG. 4. The measured speeds U plotted against the theoretical speeds U_{2L} predicted by Eq. (5). Experiments were categorized according to values of ϵ and Δ as indicated by the legend. The line $U = U_{2L}$ is plotted and shows that for all cases the observed speed of the intrusion was less than the speed predicted by rectilinear theory. A characteristic vertical error bar is shown in the lower left corner of the plot.

Figure 4 shows the measured intrusion speeds plotted as a function of the theoretically predicted speed, U_{2L}, given by Eq. (5). Experiments were distinguished according to Δ and ϵ, as indicated by the legend. The dashed line, $U = U_{2L}$, shows that the speeds predicted for rectilinear intrusions were higher than the measured speeds for all of the experiments. Applying linear regression revealed that $U = (0.72 \pm 0.04)U_{2L}$. The standard error in slope may be deceptively small as a consequence of requiring the fit line to pass through zero so the root mean squared error (RMSE) is also reported. The root mean square error is given by RMSE $= \sqrt{(y - U)^2/n} = \pm 0.54$ where U is the experimentally determined value and y is the value obtained through linear regression.

An example of a continuously stratified experiment is shown in Figure 5. The partial-depth mixed region in the lock collapsed after the cylinder was extracted moving along the level of neutral buoyancy at a depth of $z_C \simeq H_m/2$ below the surface of the fluid.

The intrusion head thinned as it propagated out radially, moving at near-constant speed for approximately $3R_c$ before rapidly stopping.

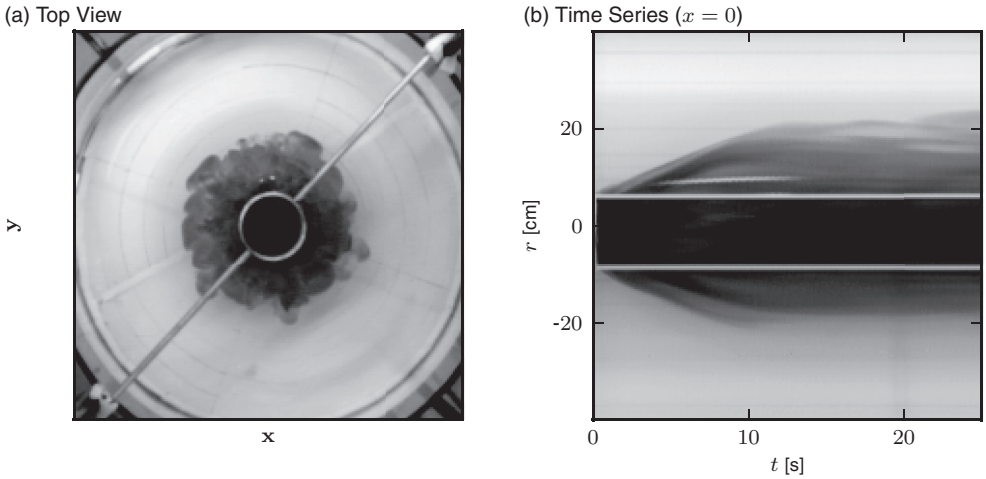

FIG. 5. Intrusion in uniformly stratified fluid shown from (a) the top view taken when $t \simeq 4$ s and (b) as a time series constructed across the diameter in the y-direction. The partial-depth lock-release experiment had $H_m = 8$ cm, $N = 1.6\,\mathrm{s}^{-1}$, and $R_c = 5.3$ cm.

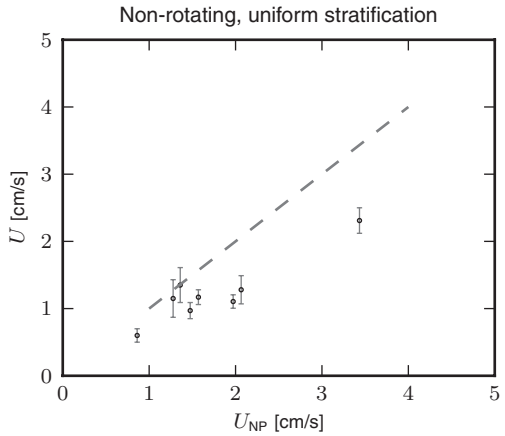

FIG. 6. The measured speeds U are plotted against the theoretical speeds given by Eq. (7). Rectilinear theory overpredicts the speed of the outgoing intrusion which is shown by the plotted line $U = U_{\mathrm{NP}}$.

Figure 6 shows the measured intrusion speeds plotted against the theoretical wave speed, U_{NP}, given by Eq. (7). The dashed line, $U = U_{\mathrm{NP}}$, shows that rectilinear theory consistently over-predicted the speeds. The slope of a best-fit line passing through the origin gives $U = (0.69 \pm 0.04)U_{\mathrm{NP}}$ (RMSE: $\pm$ 0.18). This value is consistent with the slope found for axisymmetric intrusions in non-rotating environments,[23] but is significantly smaller than the value $U \simeq 1.04U_{\mathrm{NP}}$ measured for rectilinear intrusions[12] generated by the collapse of a mixed region in stratified ambient.

The distance over which the intrusion decelerated to a halt was relatively short and a self-similar regime was not evident. Typically, R_{max} was between $1.5R_c$ and $4R_c$. Even for full-depth lock-release experiments in uniformly stratified fluid ($H_m = H$) the intrusion did not impact the side walls of the tank. Some lateral oscillations were exhibited by the patch and were attributed to interactions of the intrusions with internal waves excited ahead of the intrusion reflecting off the tank side walls as well as by internal waves generated by the return flow into the lock. However, the stopping distance was attributed to the return flow into the lock launching interfacial waves that caught up to the intrusion head. These dynamics were observed in a rectilinear geometry by Munroe *et al.*[13]

Figure 7 shows that the stopping distances were within error of the estimate, R^*, predicted through extension of Munroe *et al.*[13] who considered the time for a mode-1 wave launched by the return flow into the lock to catch up to the radial front of the intrusion. The wave was assumed to travel at speed $c = NH_m/\pi$ and traversed a distance $R_{\mathrm{max}} + 2R_c$ before reaching the front.

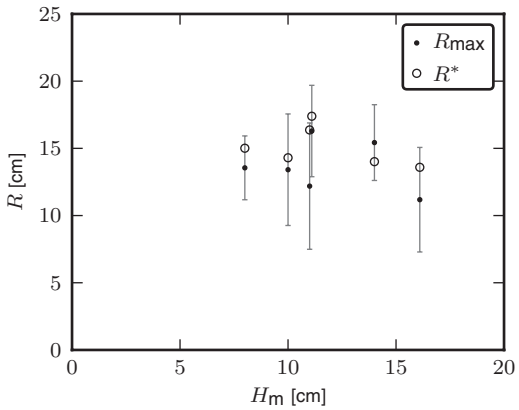

FIG. 7. The distance from the edge of the cylindrical lock, R, plotted against the height of the mixed region, H_m. The measured stopping distance of the intrusion, R_{max}, compared with the distance at which a mode-1 internal wave catches up with the front of the intrusion, R^*.

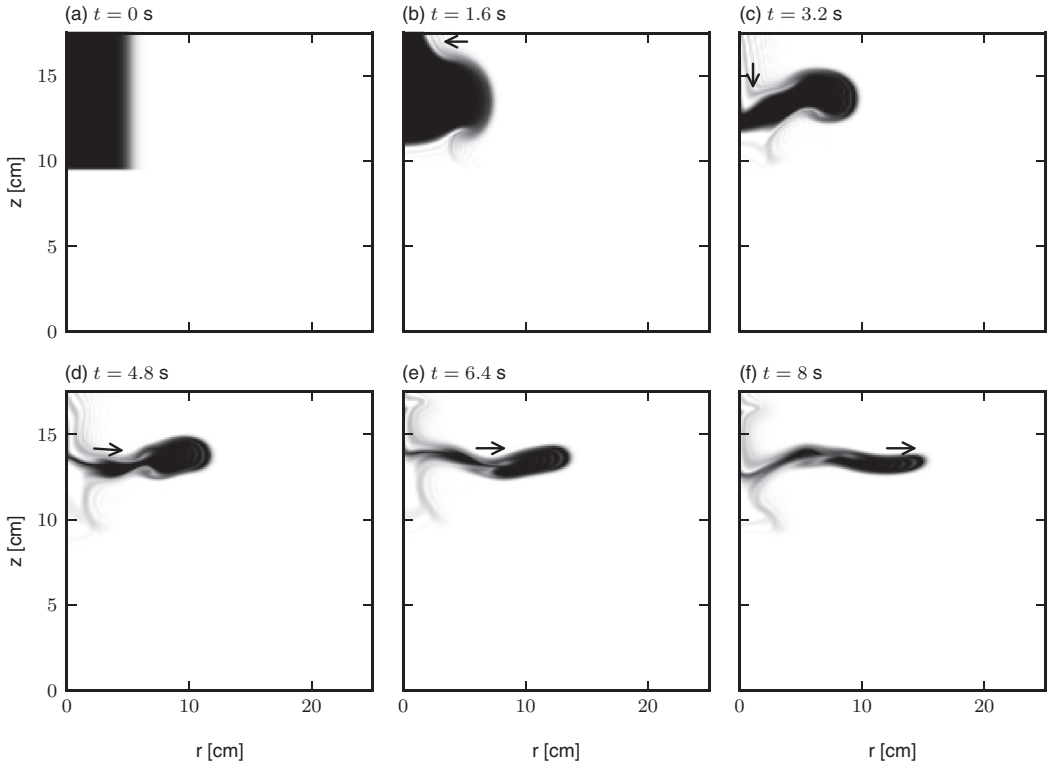

FIG. 8. Cross section of a passive tracer field constructed from a numerical model of the experiments in Figure 5. The grayscale represents the concentration and black arrows highlight the formation and subsequent motion of the interfacial wave.

Because the geometry of the experiments did not allow us to capture vertical cross sections of the flow evolution, we implemented a fully nonlinear numerical simulation to examine the internal wave catching up with the front of the intrusion. The code, described by McMillan and Sutherland,[15] solves the cylindrical Navier-Stokes equations by approximating spatial derivatives with second order finite difference and time stepping with the leapfrog method. At the free-slip boundaries the no normal flow condition is imposed.

Figure 8 shows six snapshots taken over two buoyancy periods of a simulation that was initialized with the same parameters as the experiment shown in Figure 5. At $t = 1.6$ s the black arrows highlight the motion of the return flow which sets the amplitude of the internal wave at the depth of the intrusion. In the subsequent images the black arrows indicate the motion of the internal wave launched by the return flow and which catches up to and stops the advance of the intrusion head. The time at which the wave arrives at the front of the intrusion appears to coincide with the intrusion reaching its maximum radius of propagation.

B. The effects of rotation

The qualitative nature of the collapse was noticeably different in the rotating experiments. For all experiments with significant rotation, after the initial "slumping phase," which occurred relatively quickly, the intrusion propagated out at near-constant speed, rapidly decelerated and, unlike non-rotating cases, reversed directions.

Time series taken from typical two-layer rotating experiments are shown in Figure 9. The experimental parameters were chosen to be similar to those of the non-rotating experiments in Figure 3. For each plot, the Rossby deformation radius L_D and the radius of the cylinder R_c is indicated on the right hand side.

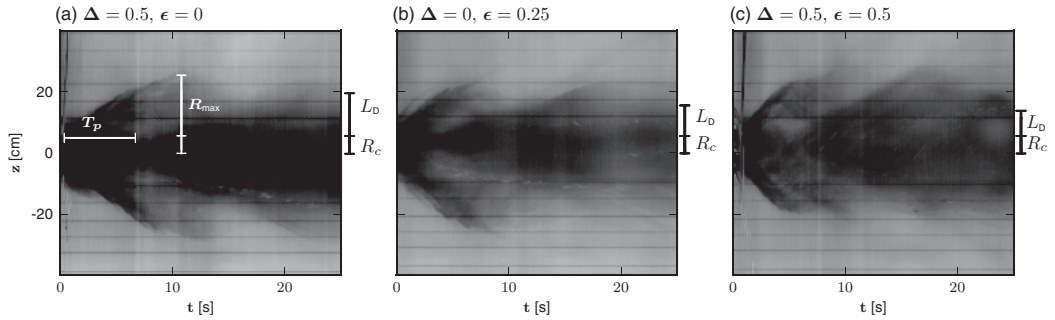

FIG. 9. Time series taken from rotating experiments in a two-layer fluid with $\Omega = 0.2\,\mathrm{s}^{-1}$, $H = 10$ cm, $R_c = 6$ cm and (a) $H_L = 2.5$ cm, $\rho_L = 1.0254\,\mathrm{g/cm}^3$, $\rho_C = 1.0186\,\mathrm{g/cm}^3$ (b) $H_L = 5$ cm, $\rho_L = 1.0254\,\mathrm{g/cm}^3$, $\rho_C = 1.0186\,\mathrm{g/cm}^3$, (c) $H_L = 2.5$ cm, $\rho_L = 1.0254\,\mathrm{g/cm}^3$, $\rho_C = 1.0050\,\mathrm{g/cm}^3$. In (a) the oscillatory period, T_p, measured as the time between the first and second outward pulse and the maximum radius of propagation, R_{max} are shown.

Figures 9(a) and 9(b) show experiments where either $\epsilon = 0$ or $\Delta = 0$. Unlike the non-rotating equivalents shown in Figure 3, the rotating intrusion did not impact the side wall of the tank. Instead, the direction of flow reversed abruptly. In the cases for which ϵ and Δ were both non-zero (Figure 9(c)) a longer period of deceleration was apparent from the time series.

The two-layer experiments explored moderate values of the Rossby number ($\mathrm{Ro} \gtrsim 1$) so that the intrusion propagated outward at near-constant speed for a measurable distance before being affected significantly by rotation. Accordingly, rotation was not expected to influence the initial speed of the intrusion.

The measured speeds are plotted against $U_{2\mathrm{L}}$ in Figure 10. The dashed line, $U = U_{2\mathrm{L}}$, shows that rectilinear theory over-predicts the speed of the intrusions. A best-fit line passing through the origin gives $U = (0.68 \pm 0.03)U_{2\mathrm{L}}$ (RMSE: $\pm$ 0.33), comparable to that measured for non-rotating cases.

The distance, R_{max}, over which the intrusion propagated before the deceleration began and the flow changed direction is illustrated by white vertical bars in Figure 9(a); it is the radial distance traversed by the intrusion from the inner edge of the cylindrical lock.

Figure 11 shows a non-dimensional plot of R_{max}/L_D against Ro. For $\mathrm{Ro} \gtrsim 2$, $R_{\mathrm{max}} \leq L_D$. However, for $\mathrm{Ro} < 2$ we found that $R_{\mathrm{max}}/L_D \in (1, 2)$. This is a smaller ratio than that observed for gravity currents propagating beneath uniform ambient.[25] Since gravity currents cannot generate

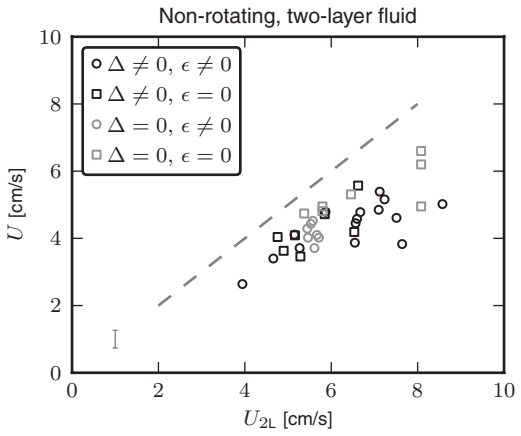

FIG. 10. For the two-layer rotating experiments, the measured speeds U are plotted against the theoretical speeds $U_{2\mathrm{L}}$ given by Eq. (5). Experiments were separated according to values of ϵ and Δ as shown in the legend. The line $U = U_{2\mathrm{L}}$ is plotted and shows that for all cases the observed speeds were less than the predicted speeds. A characteristic vertical errorbar is shown in the lower left corner of the plot.

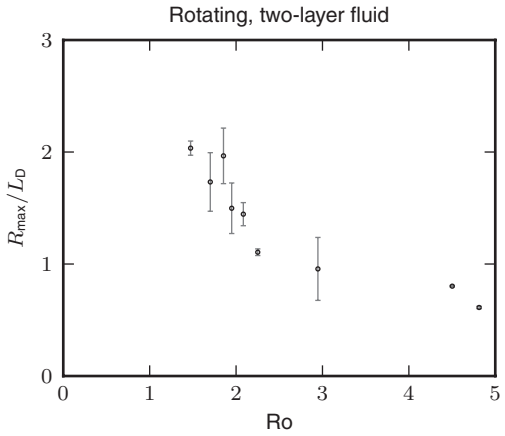

FIG. 11. For the two-layer rotating experiments, the maximum distance propagated by the intrusion, R_{max}, (illustrated in Figure 9) is normalized by the Rossby deformation radius, L_D given by Eq. (8) and plotted against the Rossby number given in Eq. (9).

internal waves, this further supports our inference that internal waves act to restrict the maximum radial distance propagated by an intrusion.

Visually tracking the concentration of dye in Figure 9 revealed regular pulsations of the intruding fluid. The dye initially concentrated in the lock moved outward after the release of the lock becoming less concentrated before reaching R_{max}. Then the dye appeared to collect near the centre of the tank once more and the second outward pulsation began.

The front of this second pulsation moved outward toward R_{max} at near-constant speed often overshooting R_{max} by a short distance. The pulsations continued as the patch adjusted to the steady state. But the dye lines gradually blurred and became more difficult to track.

The intrusion behaved in a qualitatively similar manner to a gravity current. The lens-shaped bulk of fluid expanded and contracted as it released outwardly propagating pulses. By averaging over the time between successive pulses Hallworth *et al.*[25] found $\omega = 1.05\, f_0$.

The time from the beginning of the experiment to the first outward pulse T_p is illustrated in Figure 9(a). In experiments for which T_p could be measured the corresponding frequency $\omega_p = 2\pi/T_p$ was found to increase as the rotation rate of the fluid increased so that $\omega_p = 2.8 f_0$, significantly higher than that observed for bottom propagating currents.

In the uniformly stratified experiments, the adjusting patch formed a lens-shaped structure that alternatively expanded and contracted vertically and horizontally. The top views shown in Figure 12 were taken from a full-depth lock-release experiment. In Figure 12(a) one buoyancy period had passed and the intrusion front advanced in spokes. After two buoyancy periods (Figure 12(b)) the finger-like tendrils at the leading edge wrapped around the patch as it contracted anticyclonically

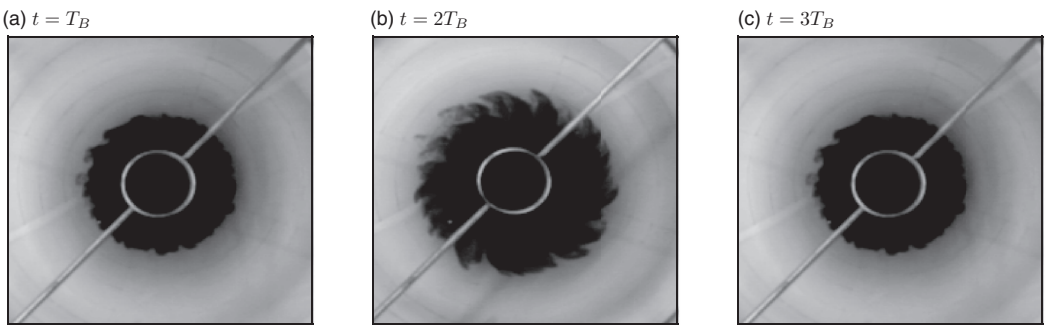

FIG. 12. The top view of a rotating full-depth lock-release experiment in uniformly stratified fluid after (a) one, (b) two, and (c) three buoyancy periods. In this experiment $H = 17.5$ cm, $\Omega = 0.3\,\mathrm{s}^{-1}$, $N = 2.27\,\mathrm{s}^{-1}$.

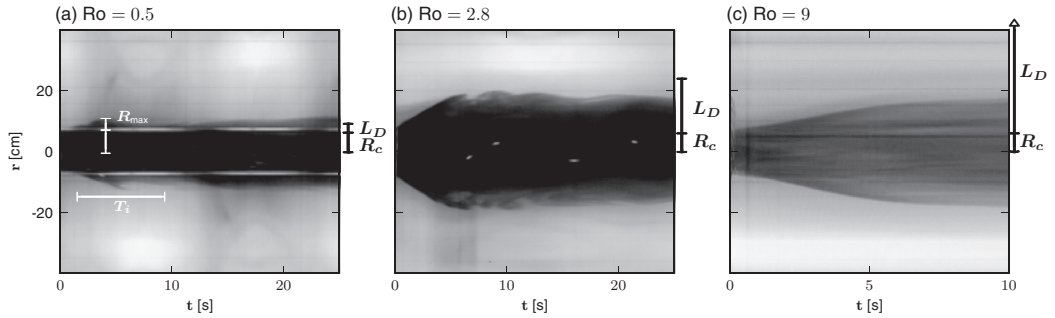

FIG. 13. Time series taken from rotating experiments in continuously stratified fluid for increasing magnitudes of the Rossby number $\mathrm{Ro} = L_D/R_c$ with $N \simeq 1.5\,\mathrm{s}^{-1}$, $R_c \simeq 5$ cm (a) $H_m = 7.5$ cm, $\Omega = 0.3\,\mathrm{s}^{-1}$ (b) $H_m = 12.7$ cm, $\Omega = 0.1\,\mathrm{s}^{-1}$, and (c) $H_m = 14.9$ cm, $\Omega = 0.03\,\mathrm{s}^{-1}$. The oscillatory period T_i is illustrated in (a) and is measured as the time between the beginning of first and second expansion.

to form an outer spiral structure. After three buoyancy periods (Figure 12(c)) the lens had expanded again and over longer times was observed to oscillate laterally as the lens rotated anticyclonically.

Particles that were placed on the surface of the lock-fluid at the start of the experiment revealed, as expected, that the ambient above the collapsed mixed layer rotated cyclonically.

Figure 13 shows radial time series for three experiments with increasing values of the Rossby number. The intrusions propagated out radially at near-constant speed for about one buoyancy period. Compared with the non-rotating experiments (e.g., see Figure 5) the initial near-constant speed phase lasted for a shorter time and the intrusion traversed a shorter radial distance.

Figure 14 shows the measured speeds plotted against the theoretical speeds as defined in Eq. (7). The dashed line, $U = U_{\mathrm{NP}}$, shows that the theory over-predicted the speeds. Consistent with the non-rotating case, $U = (0.68 \pm 0.04)U_{\mathrm{NP}}$ (RMSE $\pm$ 0.16). Rotation had no influence on the speed of the intrusion during the initial collapse phase.

In the absence of rotation we saw that the advance of an asymmetric intrusion stopped as a consequence of interactions with internal waves. Rotation additionally influenced the stopping distance for small Rossby numbers ($\mathrm{Ro} < 1$). In some cases, stopping at distances less than one lock-radius.

The time series shown in Figure 13 compares the stopping distance, R_{max}, to the Rossby deformation radius, L_D. The radius of the cylinder, R_c, is indicated on the right hand side. For $\mathrm{Ro} = 0.5$ (Figure 13(a)) a relatively short period of near-constant speed was observed. When $\mathrm{Ro} = 2.8$ (Figure 13(b)) the near-constant speed phase lasted longer. The time series clearly shows

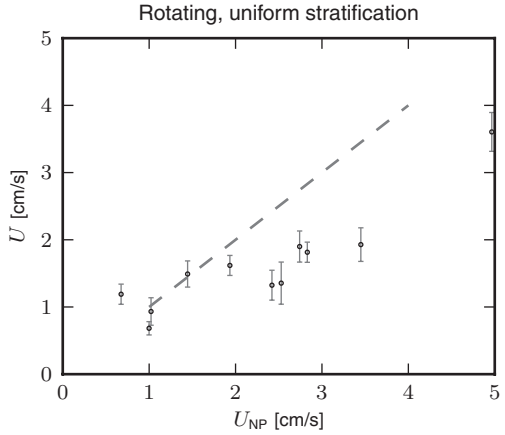

FIG. 14. For the rotating uniformly stratified experiments the measured speeds U are plotted against the speeds predicted by Eq. (7). The line $U = U_{\mathrm{NP}}$ is plotted and shows that for all cases the measured speed was less than the predicted speed.

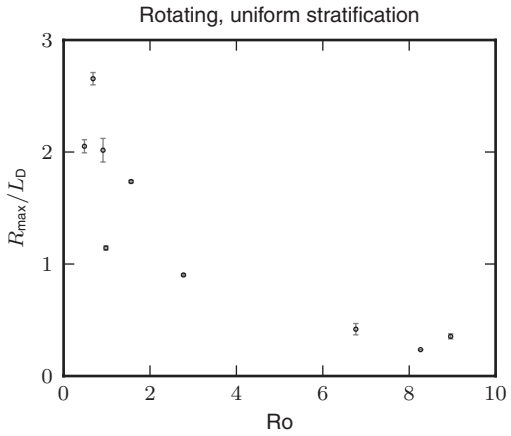

FIG. 15. For the continuously stratified rotating experiments, the maximum distance traversed by the intrusion, $R_{\max}$, (illustrated in Figure 13) is normalized by the Rossby deformation radius, given by Eq. (8), and plotted against the Rossby number, defined by Eq. (9).

the oscillatory motion of the patch as it geostrophically adjusts. Increasing the Rossby number even further to Ro = 9 (Figure 13(c)) resulted in an intrusion that behaved more similarly to the non-rotating case. The deformation radius extended beyond the radius of the tank and so the intrusion stopped moving well before the Coriolis effect could impact its motion.

For the range of Rossby numbers tested in our experiments $R_{\max}$ was between $0.7R_c$ and $3R_c$. The relationship between $R_{\max}/L_D$ and Ro is shown in Figure 15. For Ro $\lesssim 1$, $R_{\max}/L_D \in (1, 3)$. The intrusions overshot the equilibrium position as it geostrophically adjusted. In agreement with Stuart *et al.*[27] the graph shows that the maximum radius of propagation scaled with the Rossby deformation radius for small Rossby numbers (Ro > 1). For values of Ro $\gtrsim 2$ the predicted deformation radius was much larger than the recorded stopping distance since $L_D \to \infty$ as $f_0 \to 0$.

The counter-rotation of the intrusion can limit $R_{\max}$,[29] but the associated theory for an axisymmetric intrusion[31] which does not account for the influence of internal waves, over-predicted the stopping distance by a significant factor even for experiments with large Rossby numbers. The stopping distances were more accurately predicted by considering direct interactions of the intrusion with internal waves.[13]

The top views in Figure 12 and the time series in Figure 13 clearly demonstrate the oscillatory behaviour of the patch. These oscillations create a wave-like pattern in the time series. The time to the first trough, T_i, (shown in Figure 13(a)) decreased as the frequency of rotation increased.

The experiment shown in Figure 13(b) has a comparable Rossby number to the two-layer experiments shown in Figure 9. In the two-layer experiments the patch pulsated in a series of outward bursts, while in the uniformly stratified experiments the oscillations were relatively smooth and the second dilation of the patch was much shorter.

V. DISCUSSION AND CONCLUSIONS

The initial speeds of intrusions generated by the collapse of a uniform density patch in stratified fluid were found to be 65%–70% smaller than those predicted by rectilinear theory. In both two-layer and uniformly stratified fluids rotation had no significant influence on the speed of the intrusions during the initial stage of collapse for both types of stratifications.

In no experiments did we observe the characteristic features of the self-similar regime predicted for and observed in bottom propagating gravity current experiments. In the non-rotating two-layer experiments the intrusion propagated at constant speed beyond $7R_c$ if $\epsilon = 0$. For experiments with $\epsilon \neq 0$, as a result of breaking vertical symmetry a mode-1 interfacial wave was efficiently excited by the return flow into the lock. This caught up with the propagating intrusion, stalling or even halting its advance. In all the uniformly stratified experiments the intrusion, which propagated more slowly

than both mode-1 and mode-2 internal waves, stopped abruptly without reaching the tank wall. In vertically symmetric cases the intrusion halted by losing energy to the mode-2 wave that moved ahead of it. In asymmetric cases, just as in the two-layer cases, the return flow dominantly excited a mode-1 wave that was responsible for its relatively short stopping distance.

Rotation further limited the maximum propagation distance of the intrusions. Stopping distances were shorter for the rotating experiments as compared to the non-rotating cases for small Rossby numbers (Ro < 1). The stopping distance of the intrusion was a maximum of three times the Rossby deformation radius which is smaller than that observed for bottom propagating gravity currents.[25] For larger Rossby numbers the deformation radius extended beyond the radius of the tank and the stopping distance of the intrusion was influenced by interactions with the generated internal waves.

In the two-layer rotating experiments the patch periodically exhibited outward pulsations. Whereas, in the continuously stratified case the adjusting lens oscillated more smoothly about an equilibrium radius. The frequency of the oscillation of the patch increased as the rotation rate increased, but the frequency was difficult to measure accurately.

Due to restrictions of the experimental setup, this study focused upon intrusions released from locks with aspect ratios $R_c/H_m \lesssim 1$. In simulations not reported upon here it was found that the intrusion speed increased with R_c/H_m, asymptoting for $R_c/H_m \gtrsim 2$ to constant values consistent with those observed in rectilinear geometries. It is anticipated that gravity currents and intrusions emanating from locks of sufficiently large radius should initially have the speed of rectilinear intrusions; the small curvature of such locks should not influence the evolution of the slumping fluid as it approaches steady state. It is surprising that intrusions emanating from locks with aspect ratios of order unity should propagate at constant speed for distances longer than one radius. The generation of and consequent interaction of intrusions with internal waves must play a role in establishing the steady state speed. However existing theories are not readily adapted to capture these dynamics: Benjamin's theory assumes steady state from the outset and so ignores wave generation and transience associated with the collapse of a cylindrical patch of fluid; shallow water theory ignores effects associated with the generation and evolution of large amplitude, non-hydrostatic waves. Clearly more work remains to be done in theory and experiment.

ACKNOWLEDGMENTS

The authors would like to thank Branwen Price, Joshua T. Nault, and Lauren R. Blackburn for their assistance in performing some of the experiments.

[1] V. S. Maderich, G. J. F. van Heijst, and A. Brandt, "Laboratory experiments on intrusive flows and internal waves in a pycnocline," J. Fluid Mech. **432**, 285–311 (2001).
[2] J. E. Simpson and R. E. Britter, "The dynamics of the head of a gravity current advancing over a horizontal surface," J. Fluid Mech. **94**, 477–495 (1979).
[3] H. E. Huppert and J. E. Simpson, "The slumping of gravity currents," J. Fluid Mech. **99**, 785–799 (1980).
[4] T. Maxworthy, J. Leilich, J. Simpson, and E. H. Meiburg, "The propagation of a gravity current in a linearly stratified fluid," J. Fluid Mech. **453**, 371–394 (2002).
[5] T. B. Benjamin, "Gravity currents and related phenomena," J. Fluid Mech. **31**, 209–248 (1968).
[6] J. W. Rottman and J. E. Simpson, "Gravity currents produced by instantaneous releases of a heavy fluid in a rectangular channel," J. Fluid Mech. **135**, 95–110 (1983).
[7] M. Ungarish, "On gravity currents in a linearly stratified ambient: A generalization of Benjamin's steady-state propagation results," J. Fluid Mech. **548**, 49–68 (2006).
[8] M. R. Flynn and P. F. Linden, "Intrusive gravity currents," J. Fluid Mech. **568**, 193–202 (2006).
[9] D. Bolster, A. Hang, and P. F. Linden, "The front speed of intrusions into a continuously stratified medium," J. Fluid Mech. **594**, 369–377 (2008).
[10] J. Wu, "Mixed region collapse with internal wave generation in a density stratified medium," J. Fluid Mech. **35**, 531–544 (1969).
[11] J. Y. Holyer and H. E. Huppert, "Gravity currents entering a two-layer fluid," J. Fluid. Mech. **100**, 739–767 (1980).
[12] B. R. Sutherland, A. N. F. Chow, and T. P. Pittman, "The collapse of a mixed patch in stratified fluid," Phys. Fluids **19**, 116602 (2007).
[13] J. R. Munroe, C. Voegeli, B. R. Sutherland, V. Birman, and E. H. Meiburg, "Intrusive gravity currents from finite-length locks in a uniformly stratified fluid," J. Fluid Mech. **635**, 245–273 (2009).
[14] B. R. Sutherland and J. T. Nault, "Intrusive gravity currents propagating along thin and thick interfaces," J. Fluid Mech. **586**, 109–118 (2007).
[15] J. M. McMillan and B. R. Sutherland, "The lifecycle of axisymmetric internal solitary waves," Nonlinear Processes Geophys. **17**, 443–453 (2010).

[16] R. E. Britter and J. E. Simpson, "A note on the structure of the head of an intrusive gravity current," J. Fluid Mech. **112**, 459–466 (1981).
[17] R. J. Lowe, P. F. Linden, and J. W. Rottman, "A laboratory study of the velocity structure in an intrusive gravity current," J. Fluid Mech. **456**, 33–48 (2002).
[18] B. R. Sutherland, P. J. Kyba, and M. R. Flynn, "Interfacial gravity currents in two-layer fluids," J. Fluid Mech. **514**, 327–353 (2004).
[19] H. Cheong, J. J. P. Kuenen, and P. F. Linden, "The front speed of intrusive gravity currents," J. Fluid Mech. **552**, 1–11 (2006).
[20] P. Manins, "Intrusion into a stratified fluid," J. Fluid Mech. **74**, 547–560 (1976).
[21] T. Maxworthy and S. Monismith, "Differential mixing in a stratified fluid," J. Fluid Mech. **189**, 571 (1988).
[22] I. P. D. D. Silva and H. J. S. Fernando, "Experiments on collapsing turbulent regions in stratified fluids," J. Fluid Mech. **358**, 29–60 (1998).
[23] A. M. Holdsworth, S. Decamp, and B. R. Sutherland, "The axisymmetric collapse of a mixed patch and internal wave generation in uniformly stratified fluid," Phys. Fluids **22**, 106602 (2010).
[24] M. Ungarish and H. E. Huppert, "The effects of rotation on axisymmetric gravity currents," J. Fluid Mech. **362**, 17–51 (1998).
[25] M. A. Hallworth, H. E. Huppert, and M. Ungarish, "Axisymmetric gravity currents in a rotating system: Experimental and numerical investigations," J. Fluid Mech. **447**, 1–29 (2001).
[26] M. Ungarish and T. Zemach, "On axisymmetric rotating gravity currents: Two-layer shallow-water and numerical solutions," J. Fluid Mech. **481**, 37–66 (2003).
[27] G. A. Stuart, M. A. Sundermeyer, and D. Hebert, "On the geostrophic adjustment of an isolated lens: Dependence on Burger number and initial geometry," J. Phys. Oceanogr. **41**, 725–741 (2011).
[28] M.-P. Lelong and M. A. Sundermeyer, "Geostrophic adjustment of an isolated diapycnal mixing event and its implications for small-scale lateral dispersion," J. Phys. Oceanogr. **35**, 2352–2367 (2005).
[29] M. Ungarish and H. E. Huppert, "On gravity currents propagating at the base of a stratified ambient: Effects of geometrical constraints and rotation," J. Fluid Mech. **521**, 69–104 (2004).
[30] G. Oster, "Density gradients," Sci. Am. **213**, 70 (1965).
[31] M. Ungarish, *An Introduction to Gravity Currents and Intrusions* (Chapman and Hall/CRC, New York, 2009), p. 489.